INTEGRAL CONCRETE ADMIXTURE FOR WATERPROOFING AND CORROSION PROTECTION

Maximillian Desphy, **BSc. CHE, MBA**, IMRAE Corporation, Lake Elsinore, CA

Abstract: This paper describes a novel technology incorporating silicone emulsion polymers for use as an integral waterproofing admixture for concrete and for anti-corrosion protection of steel in reinforced concrete materials. The development of this product is a result of new advances in emulsification, combined with medium to high molecular weight silicone polymers. The paper aims to present the role of silicone polymers in the transformation of dicalcium and tricalcium silicates during the hydration of cement into highly rich calcium silicates, and its effect on improving the performance characteristic of concrete, and its ability to resist early stages of corrosion and water penetration. The successful development of this technology has found numerous applications in general concrete construction and served as an alternative for solvent based products containing harmful VOC's, crystalline powders, and other carcinogenic materials used in corrosion protection and waterproofing for various types of concrete structures.

The waterproofing and corrosion protection industry is a multi-billion dollar market. The commercialization of this technology has been successful with its application in GFRC (Glass Fiber Reinforced Concrete) and regular SRC (Standard Reinforced Concrete) engineering designs. The new technology stands to benefit many segments of the industry by significantly reducing the cost of maintenance, and replacement of steel reinforcements in concrete structures. A new innovative solution in waterproofing and corrosion protection that revolutionizes current industry standards.

Keywords: Integral admixture, silicone emulsions, concrete matrix, hydrophobic properties

1. **INTRODUCTION**

Improving the water resistance of concrete is an essential factor in maintaining critical performance characteristics in application areas of architectural design, elemental durability, asset protection, and environmental sustainability in various areas of construction. The new generation of integral admixtures based on silicone emulsions reacts continually during the hydration of cement "in-situ", and produces a concrete matrix that reduces the porosity through molecular bonding with silicates resulting in a denser material with greater hydrophobic characteristics.

There are three main classes of silicon compounds, which are popularly used in the hydrophobisation of concrete (see Figure 1): the silane monomer; siloxane oligomer; and polysiloxane (silicone resin). All three types form a 3-dimensional structure that is similar to the silicate component of concrete producing a stable and durable bond. Since the molecular orientation of silicon forms a tetrahedral structure, the ability to form a dimensional layer exploits this possibility with the silicon being at the center. The structural and compositional variety of such compounds originates from two facts. First, the average number of corners a tetrahedral unit shares with neighboring units, i.e. the average number of Si-O-Si bonds per silicon atom, can vary from two (as in silicones) to four (as in silica). The average degree of crosslinking is of key importance to the network structure and thus the macroscopic properties of the whole structure. The terminal groups, i.e. the groups not participating in the network formation (O-, R, etc.), modify the properties of the siloxane network. Second, as the silicon-based tetrahedra only shares corners, the structures resulting from the connected tetrahedra have many degrees of freedom and can adopt a variety of geometries, as explained by Jutzi, P. The uniqueness of its structure and reactivity extend the posibility of bonding with any organic and inorganic material, as such during the hydration of cement excess silicates of dicalcium and tricalcium silicates can be bonded with various functional groups thus creating a larger dimensional structure of many unique characteristics (see Figure 2).
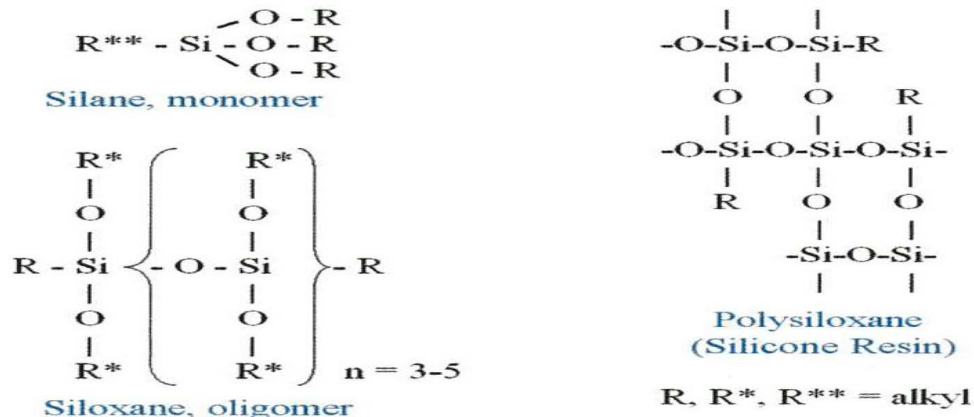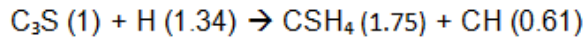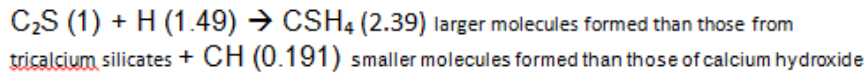

FIG. 1

Illustration of standard cement reaction with water (using standard cement chemistry abbreviation)

Tricalcium Silicate (50-70% in cement):
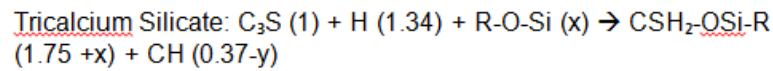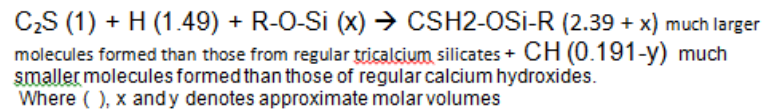
C_3S (1) + H (1.34) → CSH_4 (1.75) + CH (0.61)

Dicalcium Silicate:

C_2S (1) + H (1.49) → CSH_4 (2.39) larger molecules formed than those from tricalcium silicates + CH (0.191) smaller molecules formed than those of calcium hydroxide

Concrete Matrix:

Integral admixture reaction on hydration of cement

Tricalcium Silicate: C_3S (1) + H (1.34) + R-O-Si (x) → CSH_2-OSi-R (1.75 +x) + CH (0.37-y)

Dicalcium Silicate:

C_2S (1) + H (1.49) + R-O-Si (x) → CSH2-OSi-R (2.39 + x) much larger molecules formed than those from regular tricalcium silicates + CH (0.191-y) much smaller molecules formed than those of regular calcium hydroxides.
Where ( ), x and y denotes approximate molar volumes
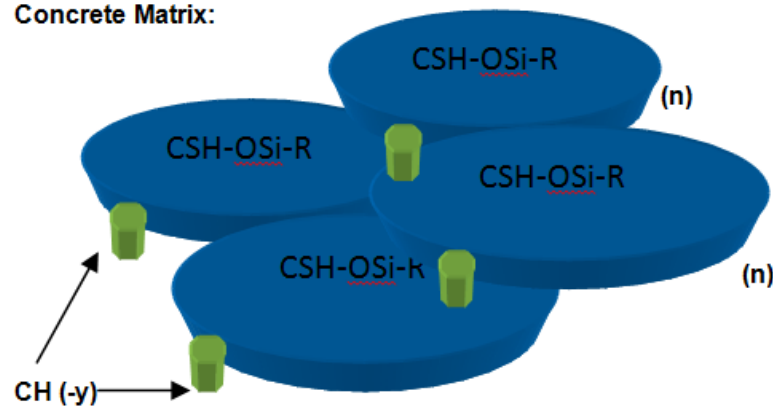
Concrete Matrix:

FIG. 2

This research in silicone admixture technology shows the benefit of adding the product in concrete mix designs, where significant properties are improved such as freeze thaw resistance, reduction of water ingress, reduction of chloride ion penetration, and corrosion protection to name a few. The silicone emulsions also contribute to the further reduction of water to cement (W/C) ratio, which increases overall physical properties of concrete in both compressive and flexural strengths. Silicone emulsion admixtures are also found to be very compatible with most types of polycarboxylate reducers, and have been observed and tested on various types of mix designs in both heavy and light weight aggregates including non-ionic to highly anionic plasticizers and/or systems, maintaining workability performance whether in SCC (self-consolidating concrete) or in traditional slump type mix designs.

The modeling system presented in this paper is to identify and understand the early life stages of corrosion under normal conditions, in which Tutti (see Figure 3) describes the corrosion life cycle in two parts: (1) initiation period in which external particles enter into the concrete cover or matrix, and (2) the propagation period, which starts when the steel depassivates. The time duration and analysis of depassivation will not be presented in this paper, which depend on other several factors such as the diffusion of chlorine, temperature, and the effect of alkalinity in the environment.
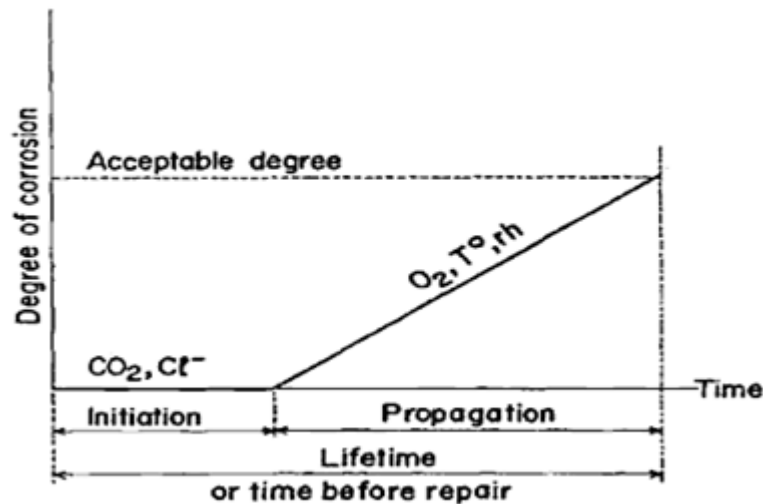

FIG. 3

A concentrated study is presented using an SCC concrete mix design of varying water to cement ratio of samples immersed at various levels of chloride concentration under normal atmospheric condition and with pH alkalinity of 7.2-8.5. The samples were evaluated by measuring the corrosion potential property of the embedded uncoated rebar using half-cell technique based on ASTM C-876, and by performing the Mohr's titration technique based on ASTM C-1152, quantitatively measuring the adsorption of chloride ion concentration in the concrete matrix and qualitatively observing color changes. In addition, measurement of water absorption and compressive strength properties are presented in this paper.

3

The samples characterized were immersed completely for 1 and 2 years in both low and high-level chloride concentrations. The principal approach was derived from ASTM B117 Neutral Salt Fog Testing, which requires atomization at 5% sodium chloride (NaCl) solution into a closed chamber maintained at 95° F and near 100% relative humidity (from the sodium chloride solution), with typical exposures lasting from 24 to 5,000 hours or longer. However, since the testing performed was conducted at regular room temperature and standard atmospheric condition, it required a longer test exposure. Many studies have shown that early initiation period up to start of the propagation period could begin as early as 120 to 360 days, and therefore based on earlier studies a two-year experiment was planned. The first test inspection was conducted after the 1st year (8,760-hours) and final inspection after the 2nd year (17,520 hours). For the conditions of the sample, a complete submersion in a closed (seal) environment under water and chloride solution shall eliminate the influence of carbonation; where the carbon dioxide from the air penetrates the concrete and reacts with the hydroxides to form carbonates, thereby reducing the pH of the concrete and thus lowering the chlorine ion needed to promote corrosion. This method attempts to determine the behavioral effects towards the submerged samples on both low and high chloride solutions without altering the normal pH of the water on a relatively low anionic environment.

3.   METHODS AND MATERIALS

Three different types of mix designs were prepared (see Table 1). A Control sample without the silicone admixture and Mix samples containing 15-ounces/sack (i.e. 94-lbs/sack of cement) of the silicone admixture added in Mix A and Mix B. The difference in Mix A and Mix B is the use of regular and recycled aggregates, respectively. In addition, Mix B has a lower W/C ratio as compared to Mix A and the Control sample. The recycled aggregates are a mixture of both coarse and fine particles and it is included to determine any effects in performance as compared to regular aggregates. A statistical analysis is presented in the paper to illustrate the difference among the three samples.

TABLE 1

Mix Design	Control (Regular Aggregates)	Mix A (Regular Aggregates)	Mix B (Recycled Aggregates)
Cement	94	94	94
Coarse Aggregate 3/8"	175	175	75
Sand	209	209	0
Recycled Aggregates (Roadbased) (coarse/fine: 50/50)	0	0	282
Water	50	50	35
Superplasticizer (Polycarboxylate)	12-ozs	12-ozs	12-ozs
Silicone Emulsion Admixture	0	**15-ozs**	**15-ozs**
Total	515	515	486
W / C Ratio	0.53	0.53	0.40
Spread	20-21"	20-21"	19-20"
Density (pcf)	142	142	111

3.1 Conditions

For this experiment sample cylinders from each mix, Control Mix, Mix A, and Mix B were prepared with four cylinders casted respectively in a 4" x 8" size container. A total of twelve cylinders were prepared according to ASTM C-31 with each of the cylinders containing three embedded Grade 40 uncoated rebar (billet) of 3/8"(d) x 3"(l) size. A set of four groups of samples were formed containing three representative samples of the Control Mix, Mix A, and Mix B. From the four equally divided groups, a set of two were immersed in a low-level chloride concentration in regular tap water with a measurable chloride concentration of 50 ppm, and the other two at a higher chloride concentration level prepared by mixing industrial NaCl at a 5% solution in de-ionized water (See Figure 4). The first two groups (i.e. Groups 1 and 2) were placed under immersion for a minimum of one year and the second group (i.e. Groups 3 and 4) for a minimum of two years.

Group 1: Three (3) cylinders submerged for 1-year in regular tap water (Chloride 50 ppm)
Group 2: Three (3) cylinders submerged for 1-year in salt water (NaCl 5% sol'n/50k ppm)
Group 3: Three (3) cylinders submerged for 2-years in regular tap water (Chloride 50 ppm)
Group 4: Three (3) cylinders submerged for 2-years in salt water (NaCl 5% sol'n/50k ppm)

3.2 Investigations

For measuring corrosion potential of uncoated rebar, a half cell copper sulfate electrode was used with a high impedance digital voltmeter, per ASTM C-876 (See Figure 6). To validate qualitatively, determination of acid soluble chloride was tested via Mohr's titration technique, per ASTM C-1152 on various locations of its cross sectional area near the rebar. A concrete sample was taken by drilling through an area within 5-mm radius of the rebar center position, and 12-mm deep from the surface area (See Figure 5). Measurement of water absorption was determined according to the BS (British Standard) 1881 Part 122:1993 to determine the rate of water absorbed at a specified time.
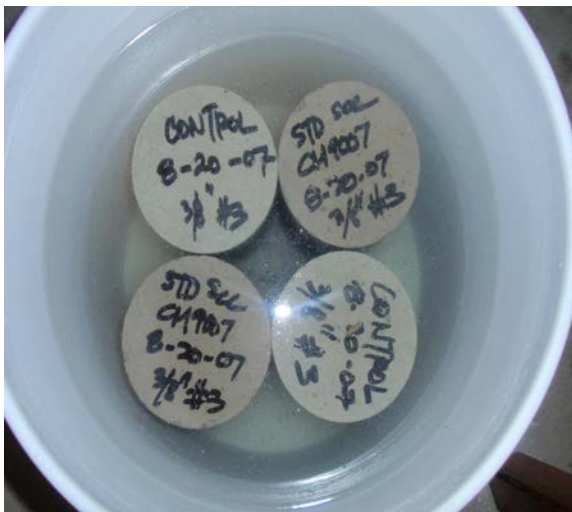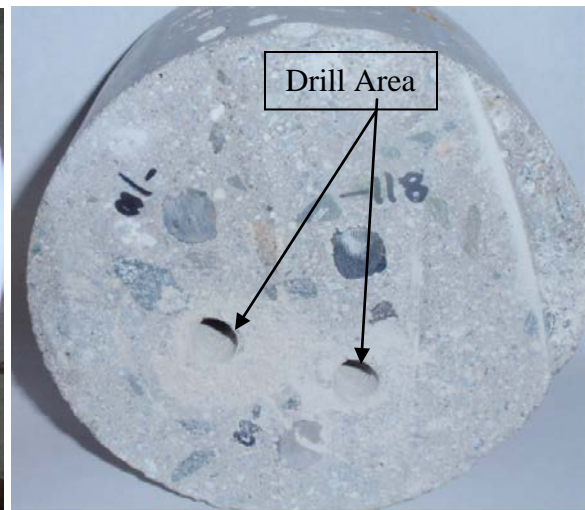

FIG. 4

FIG. 5

FIG. 6

4   RESULTS AND DISCUSSION

4.1   Measure of Corrosion Potential (ASTM C-876)

The measure of thermodynamic stability of metal in these environments provides an accurate, simple, and direct measurement on the condition of rebars, as shown on each of the following charts below. The probabilities of corrosion of carbon steel according to half-cell potential readings are based on the following conditions. More positive than -200 mV 90% probability of no corrosion; between -200 and -350 mV an increased probability of corrosion; and more negative than -350 mV 90% probability of corrosion.

Groups 1 and 2: Submerged for 1-year in regular tap water and salt-water solution (Figure 7 & 8). All mixes suggest 90% probability that no reinforcing steel is corroding in that area at the time of measurement. However, Mix A & B containing the silicone admixture are more positive indicating a lesser tendency to cause any corrosion.
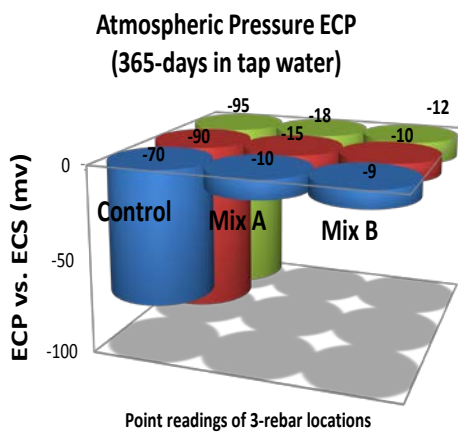

FIG. 7   **FIG. 8**
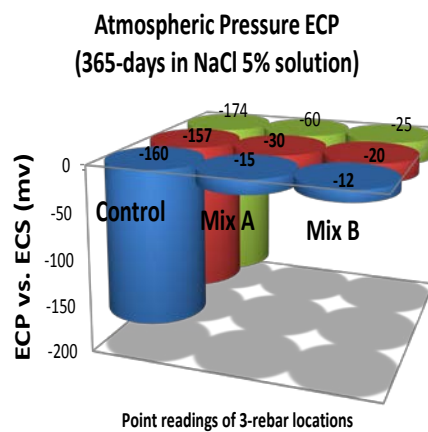
Groups 3 and 4: Submerged for 2-years in regular tap water and salt-water solution (Figures 9 & 10). Even in prolonged exposure to chloride solutions, samples containing the silicone admixture continued to exhibit reduced tendency with a 90% probability that no reinforcing steel is corroding in that area, at the time of measurement. However, at 5% or 50,000 ppm of Chloride exposure, the control sample without the admixture started to exhibit a 90% probability that corrosion is likely occurring, whereby reading more negative than -350mv at the time of measurement.
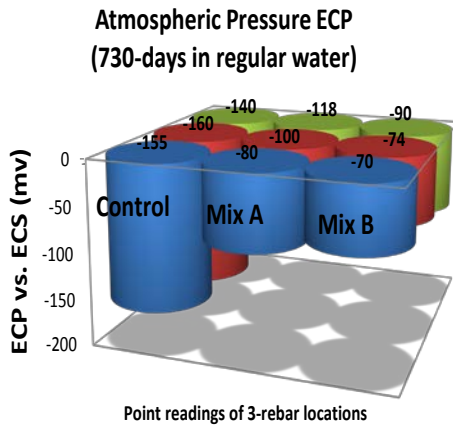
Atmospheric Pressure ECP
(730-days in regular water)

ECP vs. ECS (mv)

Point readings of 3-rebar locations

FIG. 9

Atmospheric Pressure ECP
(730-days in salt water)

ECP vs. ECS (mv)
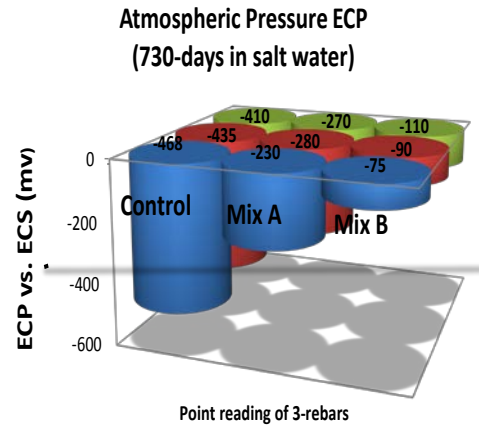
Point reading of 3-rebars

FIG. 10

4.2 Measure of Chloride Concentration via Mohr's Method in PPM (ASTM C-1152)

In order for a titrimetric method to be viable, the titration reaction (1) must be complete (i.e., titration is large) and (2) should be rapid. There are many precipitation reactions that satisfy the first requirement, but far fewer satisfy the second. Precipitation reactions of silver salts are usually quite rapid, and so argentometric titrations, which use $AgNO_3$ as the titrant, are the most common precipitation titrations. Argentometric titrations can be used to analyze samples for the presence of a number of anions that form precipitates with $Ag+$.

The Mohr Method is based on the following reaction between the titrant and the indicator:
Mohr indicator reaction $2Ag+ + CrO_4^2 = Ag_2CrO_4(s)$ titrant indicator red precipitate
The concentration of titrant rises sharply near the equivalence point, and the solubility of Ag_2CrO_4 is exceeded. The appearance of red precipitate marks the endpoint. The technique was used to measure the total acid soluble chloride of the total equivalent chloride present, by dissolving a sample in 0.5N Sulfuric Acid, and adding 5% Potassium Chromate solution as a chloride reagent, and then titrated with 2% Silver Nitrate solution. A light yellow color (see Figure 11) is exhibited on samples with a chloride content reading between 10,000-15,000 ppm, and progresses to a darker orange brown color with about 25,000 ppm of total soluble chloride (see Figure 12).

FIG. 11 w/ Potassium Chromate (Light Yellow)   **FIG. 12** end-point color (Orange Brown)

All samples immersed in tap water generally exhibited a lower chloride concentration reading as compared to samples immersed in 5% NaCl. Chloride concentrations measured Group 1 < Group 2 after 1-year, and Group 3 < Group 4. However, a comparison between the mix design samples as compared to the control shows a lower chloride concentration reading (See Figure 13).
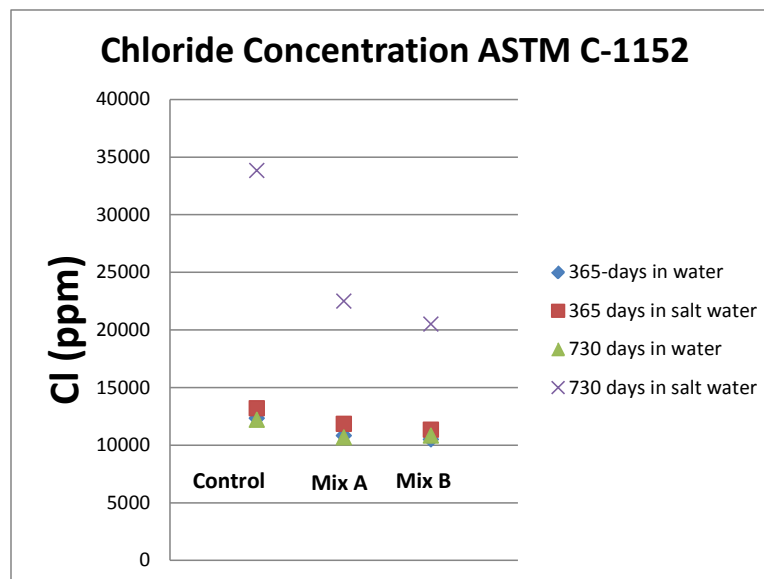

FIG. 13

Correlation between the half-cell potential readings and chloride content concentrations were determined by linear regression, as shown on Figure 14. All data suggests high correlation on increasing negative potential readings proportional to the increases in chloride content concentration.
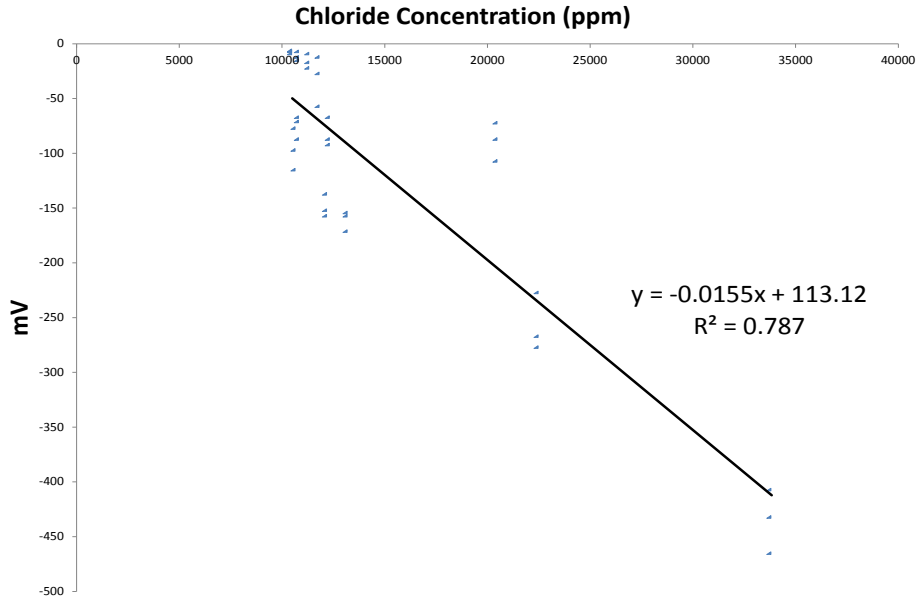
Chloride Concentration (ppm)

$$y = -0.0155x + 113.12$$
$$R^2 = 0.787$$

FIG. 14

To determine which factor(s) affected the various levels of chloride concentration and corrosion potential, an analysis of variance (ANOVA) statistical test was performed on two independent variables, the mix designs and chloride solutions respective to time, at a 95% confidence interval (CI) with α = 0.05.

The result test indicate that the four chloride solutions respective to time significantly affect the chloride concentration (see Figure 15), since F test is greater than F critical. And that the three different mix designs are insignificant to affect change, since the F test is less than F critical, respectively. Likewise, to determine which independent variable affects the difference in corrosion potential. The result indicates both chloride solutions and differences in mix designs can both affect change (see Figure 16).

Anova: Two-Factor Without Replication

SUMMARY	Count	Sum	Average	Variance			Control	Mix A	Mix B
365-days in water	3	33666	11222	953463		365-days in water	12333	10833	10500
365 days in salt water	3	36366	12122	934063		365 days in salt water	13200	11833	11333
730 days in water	3	33699	11233	708289		730 days in water	12200	10666	10833
730 days in salt water	3	76833	25611	51700963		730 days in salt water	33833	22500	20500
Control	4	71566	17891.5	1.13E+08					
Mix A	4	55832	13958	32694759					
Mix B	4	53166	13291.5	23211630					
Decision Rule:									
If F ratio is larger than F critical, then reject Ho (null hypothesis)									
If P value is less than alpha, then reject Ho (null hypothesis)									
Source of Variation	SS	df	MS	F	P-value	F crit			
Rows	4.48E+08	3	1.49E+08	15.14563	0.003316	4.757062663			
Columns	49435526	2	24717763	2.506956	0.16167	5.14325285			
Error	59158030	6	9859672						
Total	5.57E+08	11							

FIG. 15

Anova: Two-Factor Without Replication									
SUMMARY	*Count*	*Sum*	*Average*	*Variance*			Control	Mix A	Mix B
365-days in water	3	-81	-27	2675.029		365-days in water	-85	14.33	-10.33
365 days in salt water	3	-217.67	-72.5567	6290.23		365 days in salt water	-163.67	-35	-19
730 days in water	3	-329	-109.667	1436.952		730 days in water	-151.67	-99.33	-78
730 days in salt water	3	-790	-263.333	29937.33		730 days in salt water	-438	-260	-92
Control	4	-838.34	-209.585	24385.72					
Mix A	4	-380	-95	14265.6					
Mix B	4	-199.33	-49.8325	1694.199					
ANOVA									
Source of Variation	*SS*	*df*	*MS*	*F*	*P-value*	*F crit*			
Rows	94611.72	3	31537.4	7.160817	0.02081	4.757062663			
Columns	54254.25	2	27127.12	6.15946	0.035136	5.14325285			
Error	26424.84	6	4404.14						
Total	175290.8	11							

FIG. 16

A test by ANOVA was used to determine whether the difference between mix designs A & B has an effect on chloride concentration, due to its varying W/C ratio and the use of regular and recycled aggregates respectively. The resulting test indicates that the four chloride solutions respective to time significantly affect the difference of the chloride concentration, since the F test is greater than F critical. However, the mix designs are insignificant to affect change, since the F test is less than F critical at 95% CI with α = 0.05 (see Figure 17).

Likewise, to determine if the difference between mix designs A & B has an effect on the corrosion potential. The test by ANOVA determines that both independent variables are insignificant to affect change in the corrosion potential, since their F-Test is less than F critical at 95% CI with α = 0.05 (see Figure 18).

Anova: Two-Factor Without Replication								
SUMMARY	*Count*	*Sum*	*Average*	*Variance*			Mix A	Mix B
365-days in water	2	21333	10666.5	55444.5		365-days in water	10833	10500
365 days in salt water	2	23166	11583	125000		365 days in salt water	11833	11333
730 days in water	2	21499	10749.5	13944.5		730 days in water	10666	10833
730 days in salt water	2	43000	21500	2000000		730 days in salt water	22500	20500
Mix A	4	55832	13958	32694759				
Mix B	4	53166	13291.5	23211630				
Decision Rule:								
If F ratio is larger than F critical, then reject Ho (null hypothesis)								
If P value is less than alpha, then reject Ho (null hypothesis)								
Source of Variation	*SS*	*df*	*MS*	*F*	*P-value*	*F crit*		
Rows	1.66E+08	3	55471074	127.4275	0.001164	9.276628153		
Columns	888444.5	1	888444.5	2.040924	0.248437	10.12796449		
Error	1305945	3	435314.8					
Total	1.69E+08	7						

FIG. 17

Anova: Two-Factor Without Replication							Mix A	Mix B
SUMMARY	Count	Sum	Average	Variance			Mix A	Mix B
365-days in water	2	4	2	304.0578		365-days in water	14.33	-10.33
365 days in salt water	2	-54	-27	128		365 days in salt water	-35	-19
730 days in water	2	-177.33	-88.665	227.4845		730 days in water	-99.33	-78
730 days in salt water	2	-352	-176	14112		730 days in salt water	-260	-92
Mix A	4	-380	-95	14265.6				
Mix B	4	-199.33	-49.8325	1694.199				
Decision Rule:								
If F ratio is larger than F critical, then reject Ho (null hypothesis)								
If P value is less than alpha, then reject Ho (null hypothesis)								
Source of Variation	SS	df	MS	F	P-value	F crit		
Rows	37188.06	3	12396.02	3.478336	0.166607	9.276628153		
Columns	4080.206	1	4080.206	1.14491	0.363056	10.12796449		
Error	10691.34	3	3563.779					
Total	51959.6	7						

FIG. 18

Further analysis by multiple linear regressions can predict the timeline when corrosion at 90% probability begins to occur, by combining the following sample data. The Control Mix has a 90% predicted probability that corrosion will begin to occur in 3-years at 50 ppm (low) chloride concentration and about 2 years at 50,000 ppm (high) chloride concentration, see Figure 19.
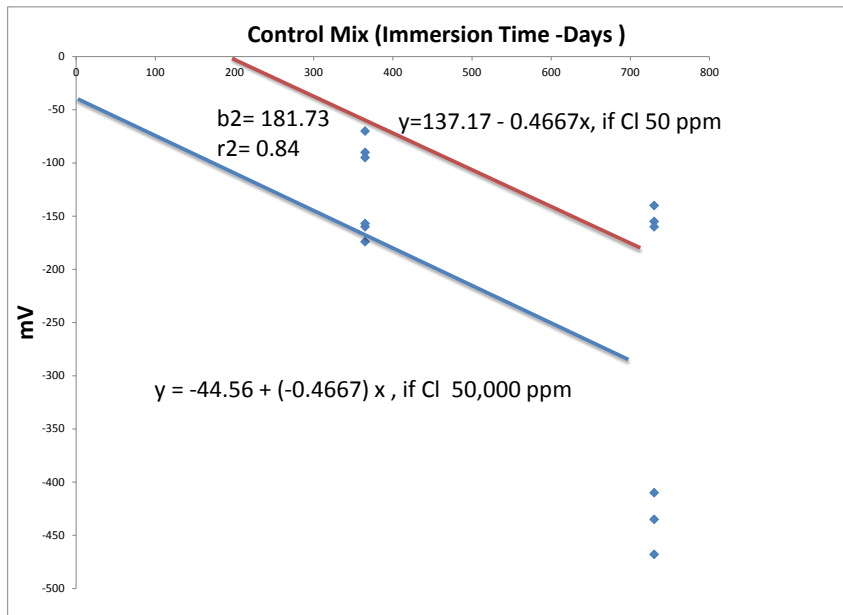

FIG. 19

Mix A has a 90% predicted probability that corrosion will begin to occur in about 4 years at 50 ppm (low) chloride concentration and about 3 years at 50,000 ppm (high) chloride concentration, see Figure 20.
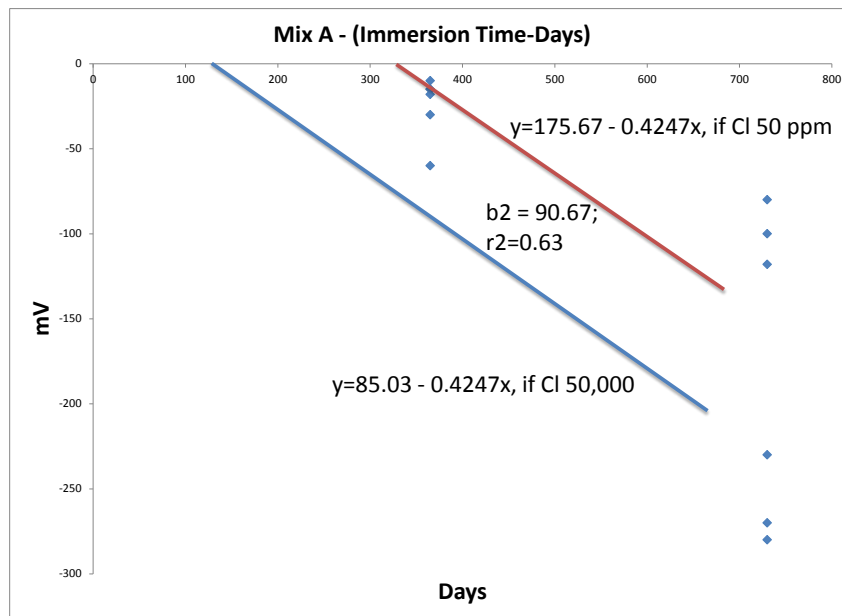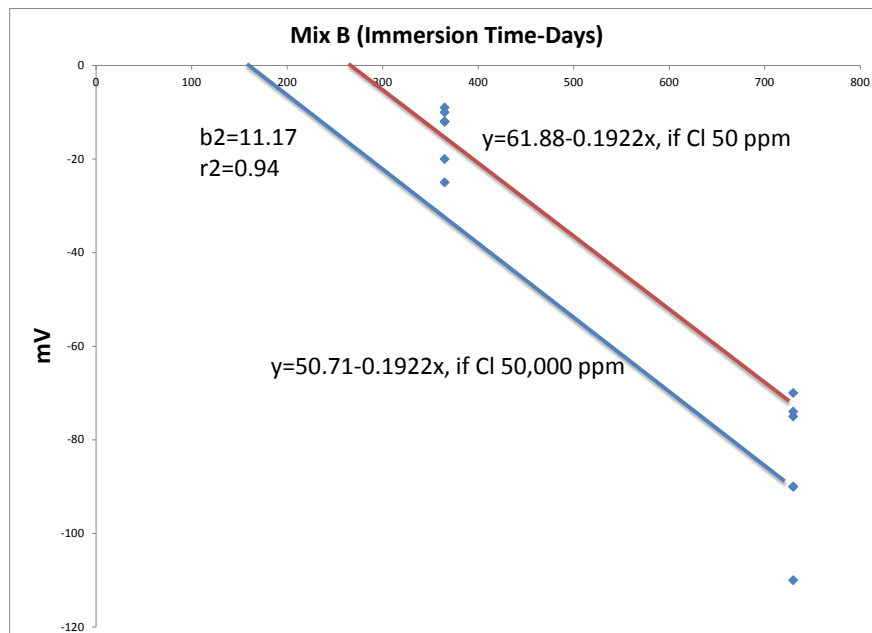

FIG. 20

Mix B has a 90% predicted probability that corrosion will begin to occur in about 6 years at 50 ppm (low) chloride concentration and about 5 years at 50,000 ppm (high) chloride concentration, see Figure 21.

FIG. 21

4.3   Topography analysis of the surface by SEM (Scanning Electron Microscope)

Samples were initially coated to prevent absorption of electron beams by sputtering or coating with Au and Pd as conductive metals (see Figures 22-23).
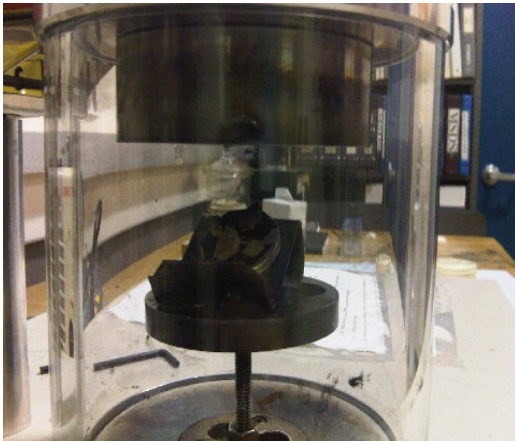

FIG. 22   **FIG. 23**
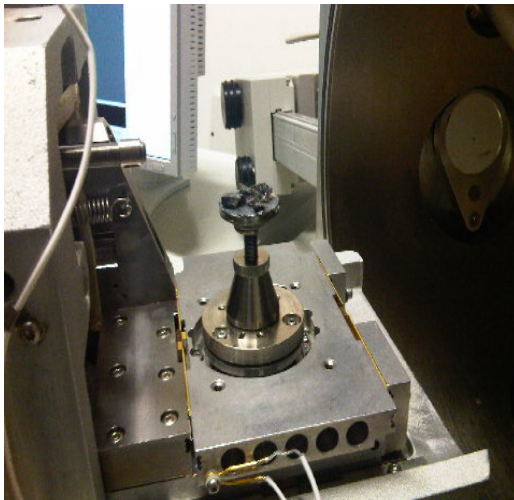
Instrument: SEM 300 Philips, see Figures 24-25 for set-up

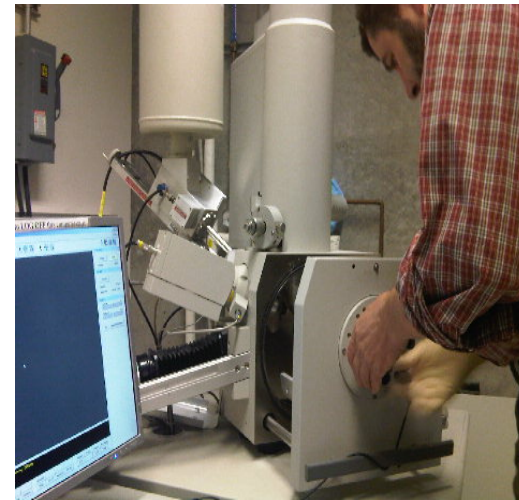**FIG. 24**   **FIG. 25**

The morphology of the surface of Mix A containing the silicone admixture shows a smoother plane (see Figure 26) and the jagged subsurface (see Figure 27) is a typical characteristic of a highly rich calcium silicate (foil like) structures, wherein readings indicate high detection of elemental calcium, see Figure 28.
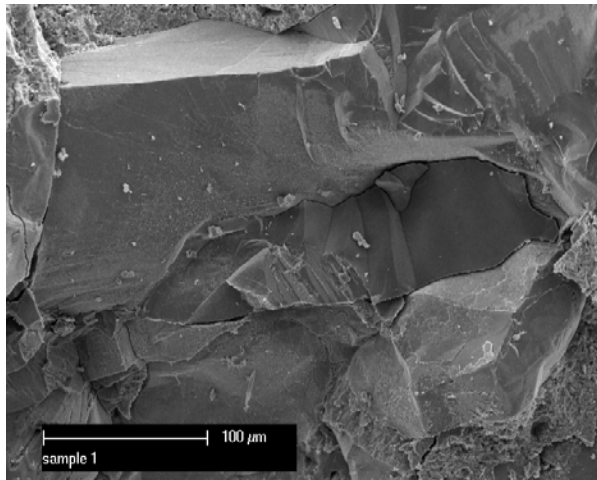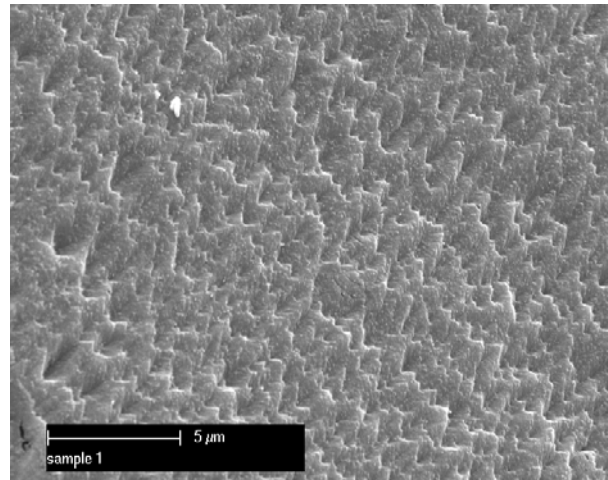
FIG. 26

FIG. 27

Mix A

```
EDAX ZAF Quantification, Standardless,
Oxygen By Diff.
SEC Table : User

Element, Wt %, At %, K-Ratio

C K,   6.85, 12.00, 0.0202
NaK,   0.56,  0.51, 0.0024
MgK,   1.17,  1.01, 0.0070
AlK,   2.56,  1.99, 0.0179
SiK,   9.31,  6.97, 0.0743
ClK,   1.12,  0.67, 0.0099
K K,   0.37,  0.20, 0.0035
CaK,  31.01, 16.27, 0.2911
FeK,   1.58,  0.59, 0.0134
Oxygen, 45.481, 59.788

Element, Net Inte., Bkgd Inte., Inte. Error, P/B

C K,    10.11,      1.13,       4.55,      8.94
NaK,     3.31,      6.63,      16.11,      0.50
MgK,     9.37,      8.65,       7.21,      1.08
AlK,    22.97,      9.13,       3.66,      2.52
SiK,    86.36,     10.09,       1.56,      8.56
ClK,     8.63,      5.94,       6.87,      1.45
K K,     2.45,      4.39,      17.90,      0.56
CaK,   178.70,      3.70,       1.00,     48.30
FeK,     2.93,      1.92,      11.62,      1.53
```

Mix B

```
 EDAX ZAF Quantification, Standardless,
 Oxygen By Diff.
SEC Table : User

 Element, Wt %, At %, K-Ratio

 C K, 12.72, 19.71, 0.0435
 NaK,  1.06,  0.86, 0.0046
 MgK,  1.69,  1.30, 0.0099
 AlK,  1.50,  1.03, 0.0102
 SiK,  6.71,  4.45, 0.0529
 K K,  0.73,  0.35, 0.0069
 CaK, 18.73,  8.70, 0.1753
 TiK,  1.47,  0.57, 0.0122
 FeK,  1.71,  0.57, 0.0144
 Oxygen, 53.684, 62.465

 Element, Net Inte., Bkgd Inte., Inte. Error, P/B

 C K,       31.27,        1.33,        2.43,       23.53
 NaK,        9.01,        7.75,        7.17,        1.16
 MgK,       19.36,       11.18,        4.36,        1.73
 AlK,       19.10,       11.18,        4.40,        1.71
 SiK,       89.73,       11.31,        1.54,        7.93
 K K,        6.99,        6.68,        8.43,        1.05
 CaK,      157.34,        6.30,        1.08,       24.96
 TiK,        8.21,        4.87,        6.74,        1.69
 FeK,        4.62,        2.62,        8.88,        1.76
```
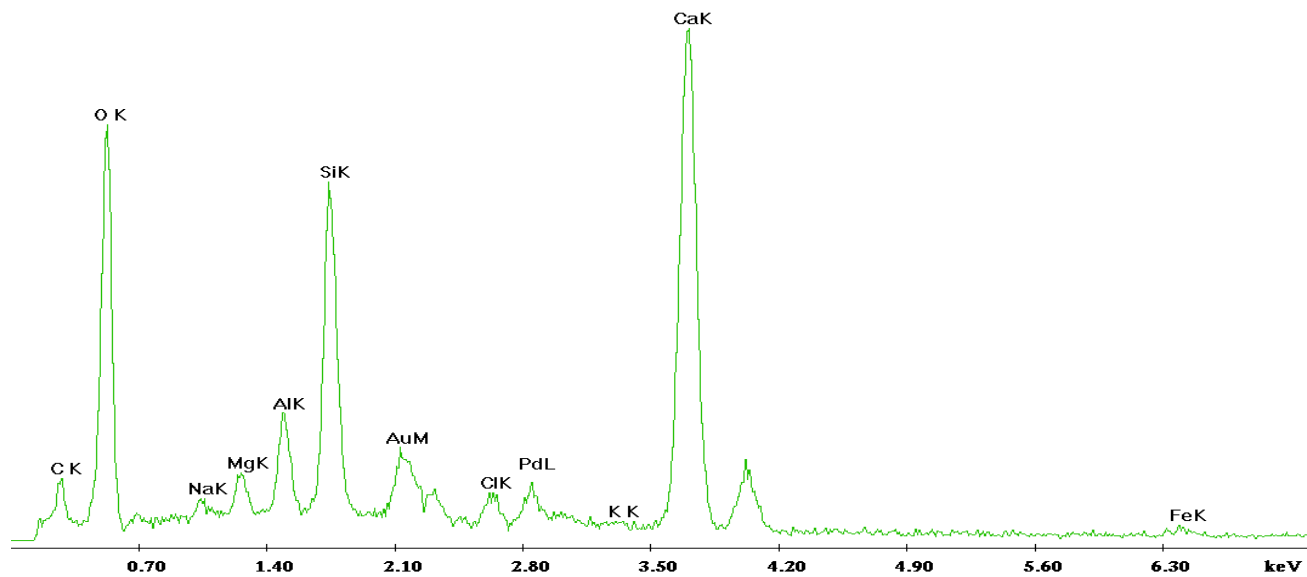
C:\users\imil\smp1-1.spc

Label A:

FIG. 28

The morphology of the surface of the Control sample that do not contain the silicone admixture, shows a rugged surface of rich calcium silicates and calcium hydroxide (hexagonal orientation) that is recognizable from the pattern, see Figures 29-30 and elemental analysis on Figure 31.
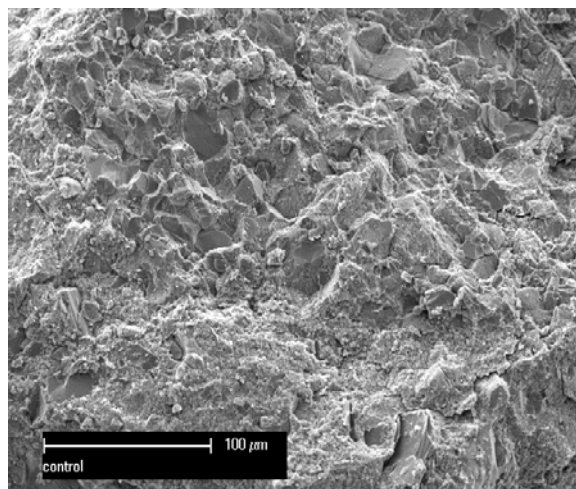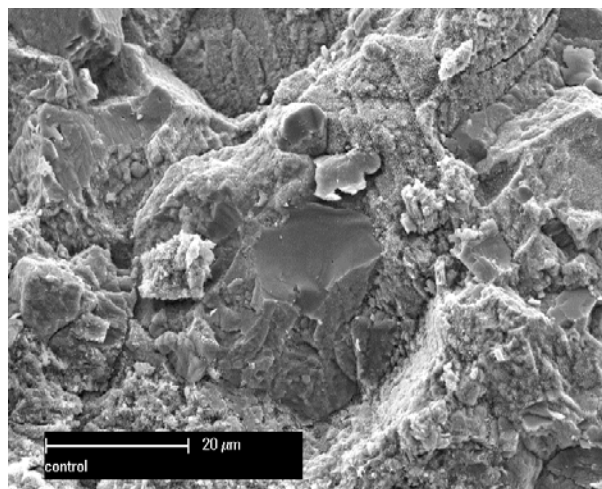

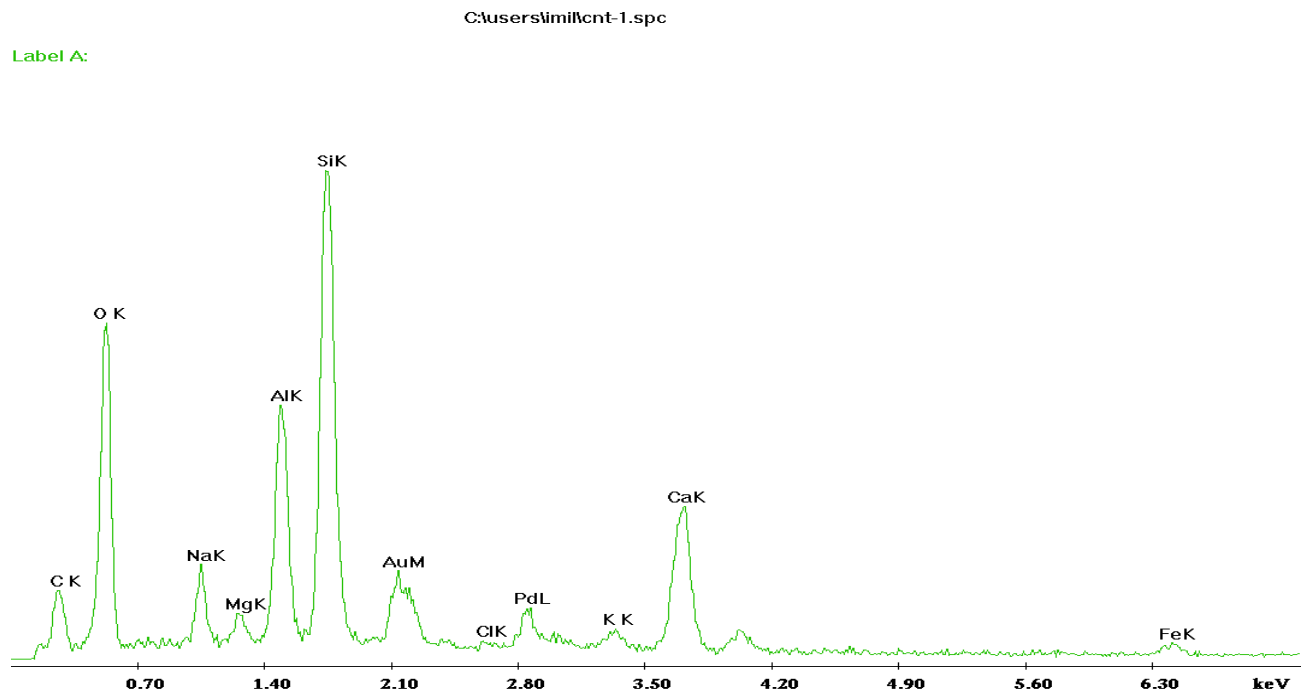**FIG. 29**

FIG. 30

Control

```
EDAX ZAF Quantification, Standardless,
Oxygen By Diff.
SEC Table : User

Element, Wt %, At %, K-Ratio

C K,   9.96, 15.42, 0.0248
NaK,   2.26,  1.83, 0.0106
MgK,   0.75,  0.57, 0.0046
AlK,   6.16,  4.24, 0.0440
SiK,  14.21,  9.40, 0.1107
ClK,   0.19,  0.10, 0.0016
K K,   0.95,  0.45, 0.0086
CaK,   8.90,  4.13, 0.0820
FeK,   2.35,  0.78, 0.0198
Oxygen, 54.278, 63.073

Element, Net Inte., Bkgd Inte., Inte. Error, P/B

C K,      13.43,        0.81,        4.02,        16.52
NaK,      15.51,        4.01,        4.35,         3.87
MgK,       6.68,        5.65,        8.83,         1.18
AlK,      60.86,        7.24,        1.98,         8.41
SiK,     138.69,        7.32,        1.24,        18.95
ClK,       1.51,        4.36,       29.39,         0.35
K K,       6.47,        3.56,        7.93,         1.82
CaK,      54.20,        3.25,        2.00,        16.67
FeK,       4.68,        1.63,        8.37,         2.88|
```
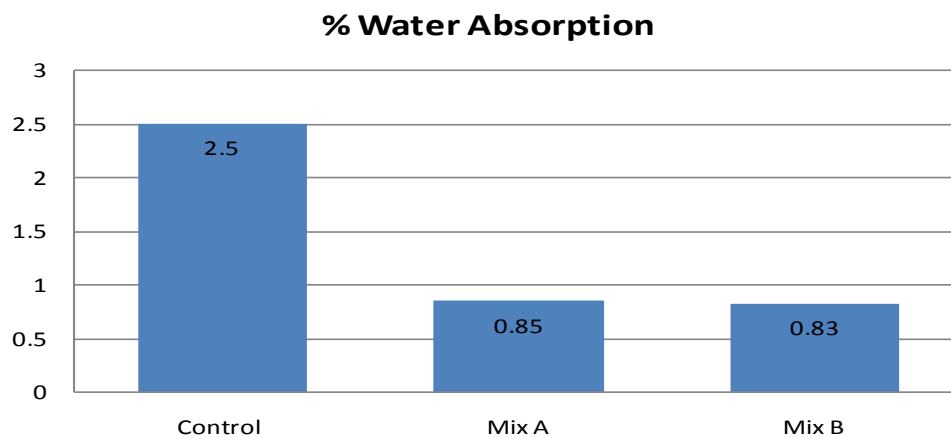
C:\users\imil\cnt-1.spc

Label A:

FIG. 31

4.4   Measure of Water Absorption (BS 1881 Part 122:1993)

The testing performed to measure water absorption shows less than 1% absorbed water for samples containing the silicone admixture, see Figure 32.

% Water Absorption

FIG. 32

4.5   Compressive Strength in Concrete (ASTM C-39)

The testing performed with various types of cements using the Control Mix and Mix A designs with W/C ratio of 0.53, shows increases in compressive strength on mixes with the silicone admixture, see Figure 33.
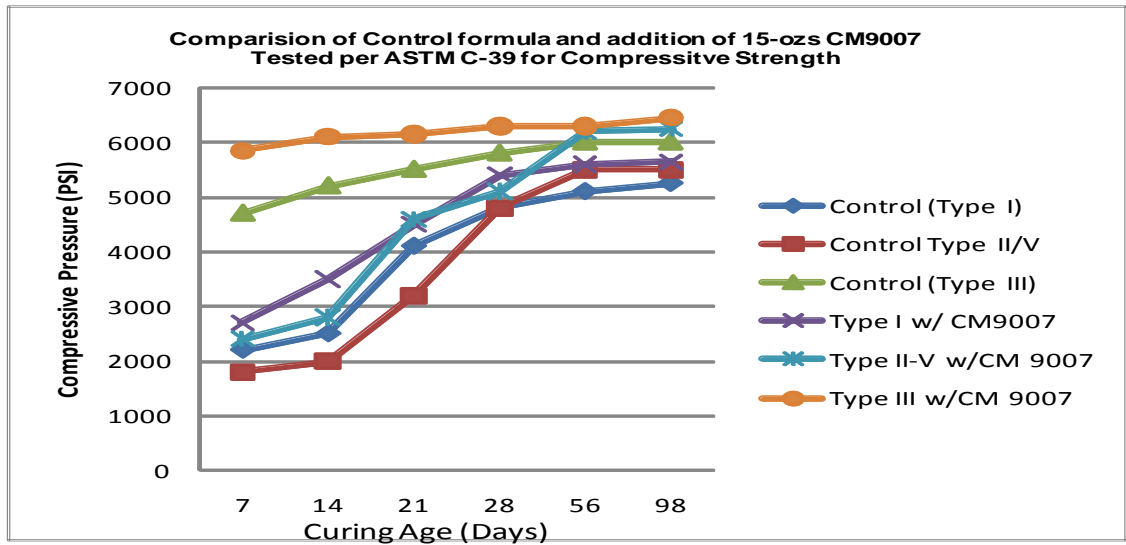

FIG. 33

5   CONCLUSIONS

The results of the study show that samples containing the silicone admixture have delayed the propagation of corrosion in concrete by extending the early stages on initiation time before active corrosion or propagation takes place. It is also apparent that between the three samples Mix A & B containing the silicone admixture have significantly extended the early life stages before active corrosion can take place. A strong correlation also exists with high concentration of chlorine at the region where high potential readings were observed, strongly suggesting that active corrosion is taking place. The observance of high detection of elemental calcium in the concrete matrix of both Mix A & B, irrespective of what aggregate was used as compared to the Control suggests efficient conversion of calcium silicates during the hydration of cement, regardless of the W/C ratio of the mix design. This has resulted to a much lower water absorption and contributed to an increase in compressive strength properties.

From this study, there are several opportunities for continued research, to understand the complete stages of the corrosion life cycle. The characterization during propagation of active corrosion should include analysis of chlorine diffusion through the concrete matrix, and its relationship to chlorine concentration. The measurement of physical strengths by accelerated ageing at elevated temperature requires examination to determine the durability and performance during this final phase period, thereby predict the active and useful life of any structural reinforced concrete.

6.   REFERENCES

Hannson, C., Poursaee, A, and Jaffer, S. (2007) "Corrosion of Reinforcing Bars in Concrete" PCA R&D Serial No. 3013, Portland Cement Association, Skokie, Illinois, USA

Highway research abstracts, Volume 24, Issues 3-4 (1991), Transportation Research Board, National Research Council, 1991

Jutzi, P. and Ulrich, S. (2003). "Silicon Chemistry: From the Atom to Extended Systems", University of Bielfeld, Germany. Wiley & Sons

Kakuda, D., Robertson, N., Newtson, D. (2005) "Evaluation of Non-Destructive Evaluation Techniques for Corrosion Detection in Concrete Exposed to a Marine Environment, University of Hawaii, College of Engineering

Masi, M., Colella, D., Radaelli, G. and Bertolini, L. (1997) Simulation of Chloride Penetration in cement-based materials, Cement and Concrete Research

Mehta, P. and Monteiro, P. (19930. "Concrete: Structure, Properties, and Materials" University of California Berkeley, Prentice Hall

Noll, W. (1968) "Chemistry and Technology of Silicones", Academic Press

Tutti, K. (1983). "Corrosion of Steel in Concrete." Report No. 4. Swedish Cement and Concrete Research Institute. Stockholm, Sweden.

White, A. (1922) Vol. 15 No. 2 "Integral Waterproofings for Concrete", University of Michigan, Ann Arbor, Michigan, Presented at the 15th Annual Meeting of the American Institute of Chemical Engineers

ASTM C31 - Standard Practice for Making and Curing Concrete Test Specimens in the Field

ASTM C39 / C39M - 12 Standard Test Method for Compressive Strength of Cylindrical Concrete Specimens

ASTM C138 / C138M - 12 Standard Test Method for Density (Unit Weight), Yield, and Air Content (Gravimetric) of Concrete

ASTM C876 - 91 Standard Test Method for Half-Cell Potentials of Uncoated Reinforcing Steel in Concrete

ASTM C1152 - Standard Test Method for Acid-Soluble Chloride in Mortar and Concrete

BS1881: Part 122: 1993 – Method for determination of Water Absorption